Effect of a disperse suspension microstructure parameters on multiple scattering characteristics at lidar sensing of seawaters

V.V. Veretennikov

Institute of Atmospheric Optics,
Siberian Branch of the Russian Academy of Sciences, Tomsk

Received September 16, 2002

Two approaches to description of lidar returns at sensing seawaters with the allowance for multiple scattering in the small-angle approximation are considered. The first approach uses an analytical relation between signal components formed due to single and multiple scattering. The second approach is based on the additive property of the signal as a function of the solid reception angle and its asymptotic properties at a large reception field of view. The lidar return characteristics describing the effect of multiple scattering are calculated with the allowance made for microphysical properties of suspended matter in seawaters. A polydisperse suspension was modeled by two fractions of particles: fine fraction of mineral origin and coarse fraction of organic origin. The results presented could be useful for planning experiments on seawater sensing in order to increase the efficiency of inverse problem solution.

Introduction

For interpretation of data on lidar sensing of seawaters, one should know analytical equations describing the relationships between the power of a lidar return and optical characteristics of the medium sounded. Such relationships can be obtained from solution of the radiative transfer equation (RTE), which describes propagation of optical radiation in the medium with the allowance for multiple scattering (MS). The specific features of seawater as a medium the optical radiation propagates through are significant light absorption at high general turbidity and high forward peakedness of the scattering phase function.[1] Under such conditions an analytical solution of the RTE can be obtained, as known,[1,2] within the framework of the small-angle approximation. This approximation is widely used for describing the behavior of lidar returns with the allowance for MS.[3–6]

The decisive factors in formation of the lidar return structure are microphysical properties of seawaters. The suspended matter in seawaters consists, as a rule, of two main fractions of different origin having different size of suspended particles. They are the coarse fraction of relatively large particles of organic origin and the fine fraction of smaller mineral particles.[1] The relative content of each of these fractions can vary widely depending on the type of seawater.

A peculiarity of light scattering in seawater is that particles of mineral origin, along with large organic particles, can contribute significantly to formation of the resultant small-angle scattering phase function.[7] In this paper we focus on the studies how the disperse composition of suspended matter in seawater affects the variability of MS characteristics of lidar returns in the small-angle approximation. The necessity of such data is dictated by the practical need in as full as possible usage of the *a priori* information on microphysical properties of a medium at interpretation of lidar experiments.

1. Analytical description of a lidar return

Based on the formalism used in Refs. 5 and 6 and taking into account the plane atmosphere–sea interface, we can write the following equation for the backscattering signal at vertical sensing of sea with a lidar from the atmosphere:

$$P(z) = P_1(z)[1 + m(z)], \qquad (1)$$

where $P_1(z)$ is the power of a lidar return in the single scattering (SS) approximation determined as

$$P_1(z) = Al^{-2}S_r\,\beta_\pi(z)\,e^{-2\tau(z)}, \quad \tau(z) = \int_0^z \varepsilon(s)\mathrm{d}s, \qquad (2)$$

as the source emits a $\delta(t)$-pulse, and the function $m(z)$ is the ratio between the MS and SS components of the lidar return. In Eq. (2) the following designations are used: $l = H + (z - H)/n_w$, where H and z are the distances from the lidar to the sea surface and to an instantaneous scattering volume in water, where single scattering occurs in the backward direction ($z > H$); n_w is the seawater refractive index, S_r is the area of the receiving aperture, $A = W(c_w/2)[T/n_w]^2$ is the instrumental constant, where W is the energy of sounding pulse; $c_w = c/n_w$ is the speed of light in water; $T = 4n_w/(1 + n_w)^2$ is the transmission coefficient at normal incidence of radiation onto the water surface. The optical characteristics of the medium that determine the behavior of the SS lidar return

0235-6880/02/12 1120-06 $02.00

$P_1(z)$ in Eq. (2) are the backscattering $\beta_\pi(z)$ and extinction $\varepsilon(s)$ coefficients. (For simplicity, atmospheric transmittance is assumed equal to unity.) Strictly speaking, Eq. (2) for the SS signal is valid for the far reception zone.[5] In the case that the optical axes of the source and receiver are matched, the far reception zone is determined by the inequality $l > R_r/\gamma_r$, where R_r and γ_r are the radius of the receiving aperture and the receiver's field of view.

Consider now the function $m(z)$, whose behavior is of primary interest for us. The conditions, under which the function $m(z)$ is determined, are the following. At description of the pulse propagation from the source to the layer, where single scattering in the backward direction occurs, multiple scattering was taken into account in the small-angle approximation. In this case, it was assumed that the coefficient of directional scattering $\beta(\gamma) = \sigma x(\gamma)$ ($\gamma = \sin\theta$, θ is the scattering angle) can be presented as a sum of an intense peak of small-angle forward scattering $\beta_1(\gamma)$ and the residual term $\beta_2(\gamma) = \beta(\gamma) - \beta_1(\gamma)$. This leads to natural resolution of the scattering coefficient into the components $\sigma = \sigma_1 + \sigma_2$ and the scattering phase function

$$x(\gamma) = a_1 x_1(\gamma) + a_2 x_2(\gamma) \qquad (3)$$

with the weighting factors $a_1 = \sigma_1/\sigma$ and $a_2 = \sigma_2/\sigma$.

The propagation of the signal from the medium backward to the receiver was described based on determination of the radiation field of a pulsed isotropic source using the Green's function method and the optical reciprocity theorem within the framework of the small-angle approximation accepted in this study.[2,3] In this case, variation of the scattering phase function near the backward direction was ignored. In addition, it was assumed that the receiver's sensitivity function with respect to the angular coordinate has circular symmetry and a stepwise shape. Finally, we neglected the size of the exit aperture and the angular divergence of sounding beam as compared to the analogous parameters of the receiver. Then in the case, when the receiver's and source's optical axes are matched, at rather small values of R_r in the far reception zone, the function $m(z)$ is determined from the following equation:

$$m(z) = l\gamma_r \int_0^\infty J_1(\nu l\gamma_r)[e^{g(\nu)} - 1]\, d\nu, \qquad (4)$$

where

$$g(\nu) = 2\int_0^z \sigma_1(z - s)\tilde{x}_1(\nu s)\, ds, \qquad (5)$$

$\tilde{x}_1(\cdot)$ is the Hankel transform of the small-angle scattering phase function:

$$\tilde{x}_1(p) = 2\pi \int_0^\infty \gamma J_0(p\gamma)\, x_1(\gamma)\, d\gamma. \qquad (6)$$

In Eqs. (4) and (6) $J_0(\cdot)$ and $J_1(\cdot)$ are the first-kind Bessel functions of the zero and first order, respectively. The right-hand side of Eq. (4) is identical to the equation describing the ratio of fluxes of scattered and non-scattered radiation passing through a circular plate with the radius $l\gamma_r$ at forward propagation of radiation from a point unidirectional stationary source of unit power in a fictitious medium, whose scattering and extinction coefficients are doubled as compared to their true values.

The ratio $m(z, \gamma_r)$ in Eq. (4) is a monotonically increasing function of the angle γ_r, and at $\gamma_r \to \infty$ it tends to the limit

$$m_\infty(z) = \exp[2\tau_{1,sc}(z)] - 1, \qquad (7)$$

independent of the shape of scattering phase function, where $\tau_{1,sc}(z) = \int_0^z \sigma_1(s)ds$ is the optical thickness of small-angle scattering. From the properties of the function $m(z, \gamma_r)$, it follows that already at the optical depth due to scattering equal to unity the fraction of multiply scattered radiation in the lidar return can significantly exceed the contribution due to single scattering, if the field of view γ_r is large enough.

2. Asymptotic properties of a lidar return

The asymptotic property of the function $m(z, \gamma_r)$ expressed by Eq. (7) allows one to write the following equation for the lidar return in the case of unlimited field of view of a receiver $\gamma_r \to \infty$:

$$P_\infty(z) = Al^{-2} S_r \beta_\pi(z) e^{-2[\tau(z) - \tau_{1,sc}(z)]}. \qquad (8)$$

The signal $P_\infty(z)$ is determined by the same optical characteristics of the medium, as in the case of single scattering approximation: the backscattering $\beta_\pi(z)$ and extinction $\varepsilon(z)$ coefficients, complemented with one more function, namely, the scattering coefficient $\sigma_1(z)$. Equation (8) has the structure analogous to the structure of the ordinary lidar equation (2) at substitution of the difference $\varepsilon(z) - \sigma_1(z)$ for $\varepsilon(z)$. Therefore, the methods and algorithms developed for solution of Eq. (2) can be easily expanded to solution of Eq. (8). Unlike the single-scattered signal $P_1(z)$, the signal $P_\infty(z)$ includes scattering of any order, exceeding $P_1(z)$ by $\exp[2\tau_{1,sc}(z)]$ times. As a result, as penetrating deeper into the scattering medium, the signal $P_\infty(z)$ decreases more slowly than $P_1(z)$.

Based on Eq. (8) for $P_\infty(z)$, the equation for the lidar return $P(z)$ at an arbitrary finite field of view of the receiver γ_r can be written in the form

$$P(z) = P_\infty(z)\,[1 - \Delta(z)], \qquad (9)$$

where the correction function $\Delta(z)$ describes the part of the total signal $P_\infty(z)$, which is formed in the scattering

volume located beyond the cone formed by the solid angle of reception. The function $\Delta(z)$ can be found as

$$\Delta(z) = l\gamma_r \int_0^\infty J_1(\nu l\gamma_r)\,[1 - e^{-2\tau_{1,sc}(z)+g(\nu)}]\,d\nu. \quad (10)$$

Unlike the lidar equation (1) with separation into components of different orders of scattering, Eq. (9) is separated into parts by the spatial index. In this case, the correction $\Delta(z)$ is always less than unity and tends to zero at $\gamma_r \to \infty$. Based on the asymptotic properties of the integral (10) (Ref. 5), at large fields of view γ_r, the equation for $\Delta(z)$ can be simplified:

$$\Delta(z) \cong \Delta_1(z) = -\frac{2\,\tilde{x}_1'(0)}{l\gamma_r} \int_0^z s\sigma_1(z-s)\,ds. \quad (11)$$

When using Eq. (11) in calculating lidar returns, there is no need in specifying full information about the scattering phase function. As can be seen from Eq. (11), to find the function $\Delta_1(z)$, it is necessary to know, besides the profile of the scattering coefficient $\sigma_1(z)$, only the derivative $\tilde{x}_1'(0)$ at zero.

3. Model of optical characteristics of seawater

Based on the modern ideas on the microphysical properties of seawaters,[1] the extinction coefficient ε in it can be presented by the following sum

$$\varepsilon = \sigma + (\chi_y + \chi_p) + \chi_w, \quad (12)$$

of the scattering coefficient σ and the coefficients of light absorption by yellow substance χ_y, phytoplankton pigments χ_p, and seawater χ_w. The major contribution to scattering comes from particles suspended in water. Those are of two main fractions: fine fraction of particles of mineral (terrigenous) origin with the size $r < 1 - 2$ μm and the relative refractive index of 1.15 and the coarse fraction comprising particles of organic (biogenic) origin ($r > 1$ μm) with the relative refractive index from 1.02 to 1.05. Analysis of experimental data[8] shows that the net contribution of χ_y and χ_p to the total extinction coefficient ε does not exceed 2–7%, and the single scattering albedo $\Lambda = \sigma/\varepsilon$ varies depending on the extinction coefficient. Parameterization of this dependence leads to the equation[8]:

$$\Lambda(\varepsilon) = b_1 + b_2/\varepsilon\,. \quad (13)$$

Processing of a large array of experimental data in Ref. 8 yielded the following values of the parameters $b_1 = 0.96$ and $b_2 = -0.0325$ for the radiation wavelength $\lambda = 0.55$ μm.

Consider now description of the small-angle scattering phase function. For particles suspended in seawater, the relative refractive index n is close to unity. The angular distribution of radiation scattered by "soft" particles can be described by the following approximate equation[9]:

$$\beta_1(\gamma) = K_{sc,1}(\delta)\,\beta^{(D)}(\gamma), \quad (14)$$

where $\beta^{(D)}(\gamma)$ is the angular scattering coefficient in the approximation of Fraunghofer diffraction, which is determined by the well-known Airy equation[10]:

$$\beta^{(D)}(\gamma) = r^2 J_1^2(kr\gamma)/\gamma^2, \quad (15)$$

where r is the radius of a suspended particle; $k = (2\pi/\lambda)n_w$. The factor $K_{sc,1}(\delta)$ in Eq. (14) is independent of the scattering angle and is a function of the phase shift $\delta = 2kr|m - 1|$ (m is the relative complex refractive index of the suspended matter):

$$K_{sc,1}(\delta) = 1 + \frac{4}{\delta^2}\left[1 + \left(1 + \frac{2}{\delta^2}\right)(1 - \cos\delta - \delta\sin\delta)\right]. \quad (16)$$

The physical meaning of this factor is that it determines the efficiency of small-angle scattering: $K_{sc,1}(\delta) = \sigma_1/(\pi r^2)$. In the case of large particles, at $\delta \gg 1$, it follows from Eq. (16) that $K_{sc,1}(\delta) \to 1$ and $\beta_1(\gamma) \to \beta^{(D)}(\gamma)$. As shown by estimates in Ref. 9, equation (14) describes with high accuracy the behavior of the angular scattering coefficient in the small-angle region for soft particles of almost any size. The error due to application of Eq. (14) increases as approaching the first zero of the Bessel function $J_1(\omega)$.

For soft particles of the same size, the normalized scattering phase function in the small-angle region has the same form as in the case of the Fraunghofer diffraction:

$$x_1(\gamma) = \beta_1(\gamma)/\sigma_1 = x^{(D)}(\gamma), \quad x^{(D)}(\gamma) = \frac{J_1^2(kr\gamma)}{\pi\gamma^2};$$
$$\sigma_1 = K_{sc,1}\,\sigma^{(D)}. \quad (17)$$

In the case of a polydisperse ensemble of suspended particles, this property does not keep true. For example, for the size distribution function of particle cross sections $s(r)$, the normalized scattering phase function has the form

$$x_1(\gamma) = \int_{r_{min}}^{r_{max}} x^{(D)}(\gamma, r)\tilde{f}(r)\,dr, \quad (18)$$

where the function

$$\tilde{f}(r) = K_{sc,1}(r)s(r) \Big/ \left[\int_{r_{min}}^{r_{max}} K_{sc,1}(r)s(r)\,dr\right] \quad (19)$$

is proportional to the distribution $s(r)$ with the weighting coefficient depending on the scattering efficiency factor $K_{sc,1}(r)$.

The derivative $\tilde{x}_1'(0)$ entering into the asymptotic equation (11) for the correction $\Delta(z)$ in the case of a polydisperse ensemble is determined by the equation

$$\tilde{x}_1'(0) = -2/(\pi k R_{eff})\,, \quad (20)$$

where

$$R_{\text{eff}} = \left[\int_{r_{\min}}^{r_{\max}} r^{-1} \tilde{f}(r)\, \mathrm{d}r \right]^{-1} \qquad (21)$$

is some effective particle size.

Earlier the variability of the scattering characteristics of disperse suspended media in seawater at variation of their microstructure parameters was studied numerically in Ref. 7. The small-angle scattering phase function $x_1(\gamma)$ (18) and its Hankel transform $\tilde{x}_1(p)$ (6), the small-angle asymmetry factor $a_1 = \sigma_1/\sigma$, as well as the effective particle size R_{eff} (21) were considered as such characteristics. The calculated results showed that small mineral particles, along with large organic particles, can contribute markedly to the formation of the above characteristics. The form of the scattering phase function, in its turn, determines the ratio between the components of the lidar return due to single and multiple scattering. In the case of a large field of view γ_r, the asymptotic dependence of the lidar return on the effective particle size R_{eff} manifests itself. The effect of the microstructure parameters of mineral and organic particles at different ratio of their contributions to the total extinction on the behavior of the functions $m(z, \gamma_r)$ and $\Delta(z, \gamma_r)$ will be studied in model calculations in the next section.

4. Results of numerical simulation

Model calculations of $m(z, \gamma_r)$ and $\Delta(z, \gamma_r)$ were performed for the following conditions. The water depth was sounded with a lidar located at the height $H = 300$ m above the sea surface; the return signal came from the depth of 20 m; the radiation wavelength was $\lambda = 0.532$ μm; the receiver's field of view γ_r varied from 0 to 15 mrad. As the input parameter of the model, we took the optical thickness of the layer τ, which varied from 1 to 4. The extinction ε and scattering σ coefficients were assumed depth-independent, and the relation between them was established based on Eq. (13).

In simulation of optical characteristics of the polydisperse suspended matter, the microstructure parameters were analogous to those given in Ref. 7. It was believed that suspended particles do not absorb radiation at this wavelength. The size spectrum of fine terrigenous (t) particles was described by the power law

$$s_t(r) = A_t\, r^{-\nu} \qquad (22)$$

with the exponent $\nu = 1$–4 in the size range $0.2 \le r \le 2.0$ μm. To describe the size spectrum of the coarse fraction of biogenic (b) particles, we selected a modified gamma-distribution

$$s_b(r) = A_b \left(\frac{r}{r_m} \right)^{\alpha} \exp\left\{ -\frac{\alpha}{\gamma} \left[\left(\frac{r}{r_m} \right)^{\gamma} - 1 \right] \right\} \qquad (23)$$

with the variable modal radius $r_m = 5$–20 μm and fixed parameters $\alpha = 8$ and $\gamma = 3$. The weighting factors A_t and A_b in the distributions $s_t(r)$ and $s_b(r)$ were chosen such that they provide for the given ratio $\xi = \sigma_b/\sigma_t$ between the contributions of these fractions to the total scattering coefficient $\sigma = \sigma_t + \sigma_b$.

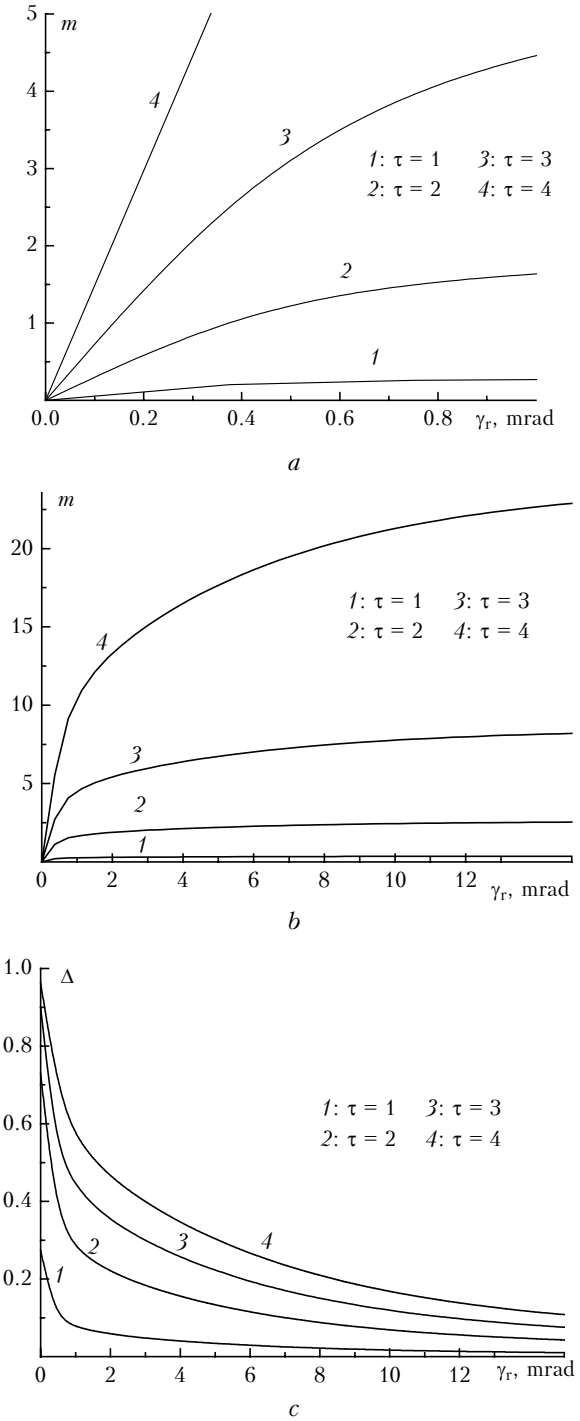

Fig. 1. Dependences of $m(\gamma_r)$ (*a*, *b*) and $\Delta(\gamma_r)$ (*c*) on the receiver's field of view γ_r for a homogenous seawater layer with different optical thickness at the depth of 20 m containing suspended particles of two fractions of mineral and organic origin.

Figures 1*a* and *b* depict the behavior of the function $m(\gamma_r)$ at variation of the optical thickness of the layer. For the results presented, the contribution $p = \sigma_t/\sigma$ of the t-fraction to the total scattering coefficient is equal to 0.2. The microstructure parameters of the fractions (22) and (23) were taken the following: $\nu = 2$ and $r_m = 15$ μm.

It can be seen from Figs. 1*a* and *b* that at the optical thickness $\tau = 1$ single scattering in the lidar return signal prevails at any γ_r, since $m(\gamma_r) < m_\infty = 0.38$. As the optical thickness increases, the contribution of multiple scattering increases and already at $\tau > 2$ it begins to prevail ($m(\gamma_r) > 1$) if $\gamma_r > 0.4$ mrad. For $\tau = 4$ at the same γ_r the value of $m(\gamma_r)$ achieves six and higher. The corresponding dependences of the function $\Delta(\gamma_r)$ for different values of the optical thickness τ are shown in Fig. 1*c*. The function $\Delta(\gamma_r)$ decreases monotonically with the increasing γ_r and increases monotonically at increasing τ. It is seen from Fig. 1*c* that at $\tau < 3$ more than 80% of the scattered energy, which could be recorded in the case of unlimited receiver's field of view, come at the input of the receiving system if $\gamma_r > 5.7$ mrad.

It should be emphasized that these values are true only for the chosen set of microstructure parameters of the suspended matter and as the parameters vary, the observed pattern will change as well. The above-said is illustrated in Fig. 2. In contrast to Fig. 1, the dependences $m(\gamma_r)$ and $\Delta(\gamma_r)$ are obtained at the same value of the optical thickness $\tau = 2$ and different ratio between the fractions characterized by the parameter $p = \sigma_t/\sigma$. The case $p = 0$ (curves *1* and *1′*) corresponds to the suspended matter consisting of only large organic particles with no particles of mineral origin. The increase of p corresponds to the increasing contribution of the fine t-fraction. The small-angle scattering phase function in this case broadens (see Fig. 7 in Ref. 7). This leads to the lower rate of increase of the function $m(\gamma_r)$, and it later approaches the saturation level m_∞. As p varies from 0 to 0.7, m_∞ can be thought constant with the error no higher than 6%.

Because of broadening of the sensing beam that occurs as the forward peak in the scattering phase function decreases, the increasingly larger part of the scattered energy remains beyond the solid reception angle and thus does not come to the receiver. This manifests itself in the lower rate of the decrease of the function $\Delta(\gamma_r)$ with the increasing p (Fig. 2*b*); the dashed curves are for the dependences $\Delta_1(\gamma_r)$ calculated by the asymptotic equation (11). As is seen from Fig. 2*b*, the domain of applicability of the asymptotic approximation (11) depends on the disperse composition of the suspended matter. Thus, for example, at $p = 0$ Eq. (11) can be applied starting from small angles $\gamma_r > 0.3$ mrad, while at $p = 0.7$ it is valid only for $\gamma_r > 6$ mrad. It should also be noted that in this case the effective particle size R_{eff} determining the behavior of $\Delta_1(\gamma_r)$ (11) through the derivative $\tilde{x}_1'(0)$ (20) also changes considerably: from 14.3 μm ($p = 0$) to the value close to 1 μm ($p = 0.7$). The accuracy of the asymptotic approximation (11) increases with the increasing γ_r.

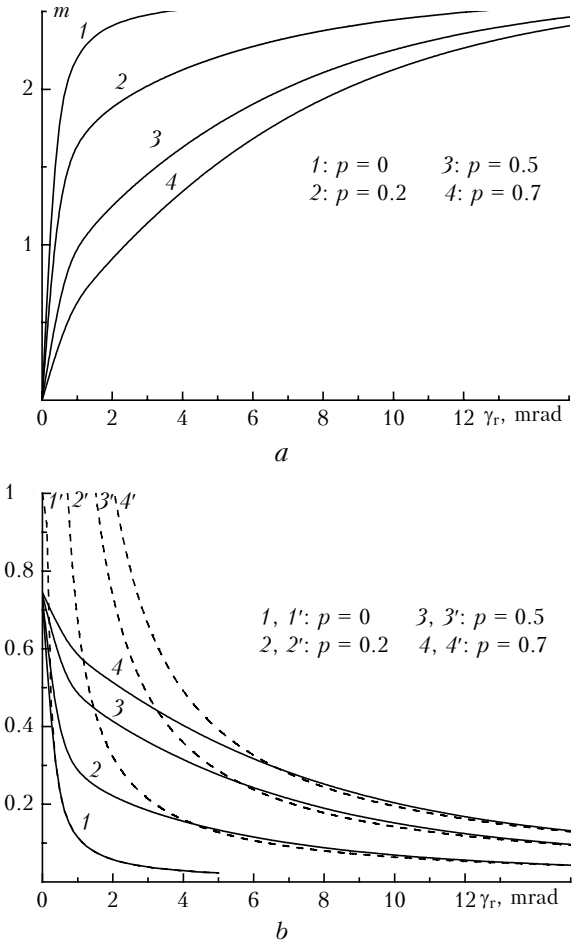

Fig. 2. Angular dependences of $m(\gamma_r)$ (*a*) and $\Delta(\gamma_r)$ (*b*, solid curves) and $\Delta_1(\gamma_r)$ (*b*, dashed curves) at different relative contribution p of the mineral fraction to the total extinction of radiation by particles and the same optical thickness of the layer $\tau = 2$.

Figure 3 shows how the parameter ν of the particle distribution for the t-fraction (22) affects the behavior of the functions $m(\gamma_r)$ and $\Delta(\gamma_r)$ at the same optical thickness of the layer $\tau = 2$ and the same relative content of both fractions ($p = 0.5$). Two regions can be separated out from the plots.

The first region determined by the angles $\gamma_r < 1$ mrad is characterized by the fast increase of the functions $m(\gamma_r)$ and decrease of the functions $\Delta(\gamma_r)$. Multiple scattering in this region is mostly formed by large particles of the b-fraction, and the effect of the t-fraction particles turns out to be weak. As a result, the discrepancy between the $m(\gamma_r)$ curves as approaching the domain boundary does not exceed 11% for all the considered values of the parameter ν. At the further increase of γ_r, the rate of change of the functions $m(\gamma_r)$ and $\Delta(\gamma_r)$ decreases. The contribution of particles of the

b-fraction to the multiple-scattered part of the signal saturates, and the discrepancy between the $m(\gamma_r)$ curves is caused by different shape of the particle distribution for the t-fraction.

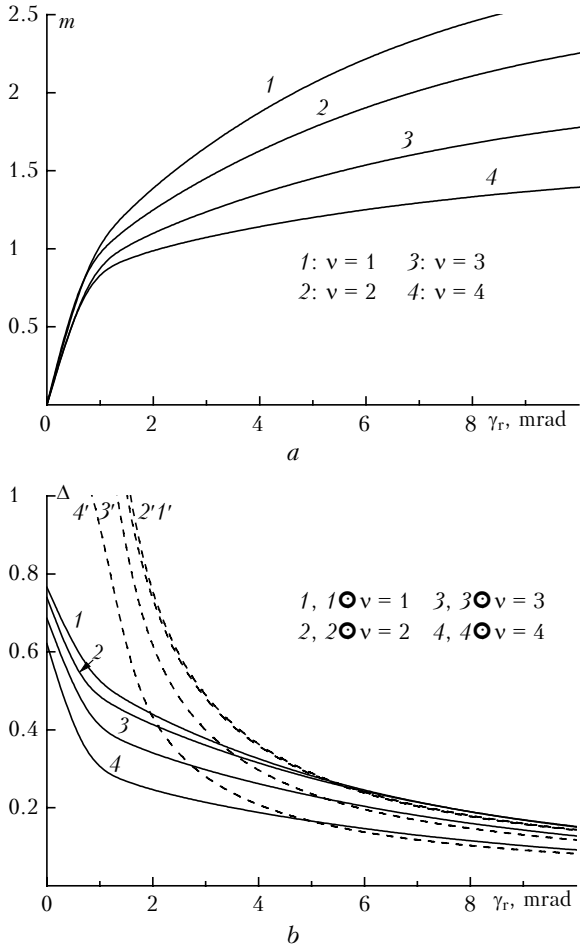

Fig. 3. Effect of the parameter ν in the distribution of particles of the mineral fraction (22) on the behavior of $m(\gamma_r)$ (*a*), $\Delta(\gamma_r)$ (*b*, solid curves), and $\Delta_1(\gamma_r)$ (*b*, dashed curves).

As follows from model calculations, the ratio between the fractions of mineral and biological particles affects more strongly the position of the lower boundary in the domain of asymptotic description of the correction $\Delta(\gamma_r)$ as compared with the variations of the distribution parameters of individual fractions. This conclusion can be illustrated by comparing Figs. 2*b* and 3*b*. The latter shows how the parameter ν affects the boundaries of applicability of the asymptotic approximation $\Delta_1(\gamma_r)$ (11). It follows from the data shown in Fig. 3*b* that the error of Eq. (11) is less than 0.4% for $\gamma_r > 5$ mrad at any values of the parameter ν.

Conclusion

An equation is formulated to describe the behavior of the lidar return signal when sounding the surface sea layer from the atmosphere as a function of optical and microphysical properties of the seawater. This equation accounts for multiple light scattering in the small-angle approximation and single scattering to large angles. The optical characteristics of the seawater include the scattering and extinction coefficients, as well as the scattering phase function in the region of small angles and in the backward direction.

Two forms of the lidar equation are considered. The first one is based on separation of the single- and multiple-scattered components in the lidar return signal. In the second form, the measured signal is considered as a part of the limited expected signal at unlimitedly wide receiver's field of view. It is shown that as the field of view increases, the dependence of the lidar return on the small-angle scattering phase function becomes less pronounced and transforms into the dependence on a single parameter, which is determined by the effective size of scattering particles.

The selected model of the small-angle scattering phase function allows the disperse composition of the suspended matter to be taken into account explicitly. The behavior of lidar signal characteristics has been studied numerically depending on the microstructure parameters of the two main fractions of particles of the mineral and organic origin at different ratio of their contributions to the total extinction. The conditions, under which information about the small-angle scattering phase function in the description of the lidar return can be replaced by a single value, namely, the effective particle size, have been evaluated. The results presented are useful in the development of methods for solution of inverse problems of the laser sensing of seawaters.

References

1. A.S. Monin, ed., *Ocean Optics*. Vol. 1. *Physical Ocean Optics* (Nauka, Moscow, 1983), 372 pp.
2. L.S. Dolin and I.M. Levin, *Handbook on the Underwater Vision Theory* (Gidrometeoizdat, Leningrad, 1991), 230 pp.
3. L.S. Dolin and V.A. Savel'ev, Izv. Akad. Nauk SSSR, Ser. Fiz. Atmos. Okeana **7**, No. 5, 505–510 (1971).
4. E.P. Zege, I.L. Katsev, and I.N. Polonskii, Izv. Ros. Akad. Nauk, Ser. Fiz. Atmos. Okeana **34**, No. 1, 45–50 (1998).
5. V.E. Zuev, V.V. Belov, and V.V. Veretennikov, *System Theory in Optics of Disperse Media* (Spektr, Tomsk, 1997), 402 pp.
6. V.V. Veretennikov, Atmos. Oceanic Opt. **12**, No. 5, 369–375 (1999).
7. V.V. Veretennikov, Atmos. Oceanic Opt. **14**, No. 2, 146–152 (2001).
8. A.N. Dorogin, O.V. Kopelevich, I.M. Levin, and V.I. Feigel's, in: *Abstracts of Reports Presented at 10th Plenum on Sea and Atmospheric Optics*, S.I. Vavilov State Optical Institute, Leningrad (1988), pp. 136–137.
9. V.I. Burenkov, O.V. Kopelevich, and K.S. Shifrin, Izv. Akad. Nauk SSSR, Ser. Fiz. Atmos. Okeana **11**, No. 8, 828–835 (1975).
10. M. Born and E. Wolf, *Principles of Optics* (Pergamon Press, New York, 1989).